Optical Properties of Host(SBA-15)-guest(AgI) Composite Materials

G. Kamalakar, Q.-Z. Zhai, Dennis W. Hwang (黃聖言), Shu-Hua Chien (簡淑華),
Yi-Han Yang (楊逸涵), Jin-Dong Lin[+] (林進東),
Yit-Tsong Chen (陳逸聰) and Lian-Pin Hwang* (黃良平)
Department of Chemistry, National Taiwan University, and Institute of Atomic and Molecular Sciences, Academia Sinica, Taipei, Taiwan, R.O.C.

Nanoclusters AgI have been prepared in the channels of SBA-15 molecular sieve host, and the host-guest nanocomposite materials were prepared by a heat diffusion method. The (SBA-15)-AgI host-guest nanocomposites were characterized by powder X-ray diffraction analysis, nitrogen adsorption-desorption isotherms at 77 K, and solid-state diffuse reflectance absorption spectra. The decrease in surface area, pore diameter, and pore volume showed the existence of silver iodide clusters in the channels of SBA-15 host. X-ray diffraction illustrates that the framework of the SBA-15 remained in the host-guest composites of (SBA-15)-AgI. As the guest loading decreases, a blue-shift was observed in the diffuse reflectance spectra. This shows that the guest existed in the channels of SBA-15 and a quantum confinement effect emerged. The photoluminescence (PL) spectra show that the PL at ~2.38 eV, associated with the hydrogen-related species, decreases substantially after the loading of AgI in SBA-15. The decrease of the PL indicates the reduction of the hydrogen concentration on the pore surface of SBA-15 after the loading of AgI guest. The intensity decrease of the self-trapped exciton (STE) band at 2.76 eV also suggests a hindrance for generating the excitons upon adding the AgI guest into the SBA-15 host.

Keywords: Optical property; SBA-15 host; AgI guest.

INTRODUCTION

The small semiconductor clusters that have hybrid molecular and bulk properties represent a new class of materials. Novel nanosized materials have been the focus of intensive investigations recently.[1] Zero-dimensional quantum dots and one-dimensional quantum wires among others have brought out many novel physical, chemical and optical properties. Zeolites are a class of porous open-framework solids with nano-channels.[2] The nano-pores of zeolites have been used as templates to create host-guest nanocomposite materials.[3-13]

Very recently, a new molecular sieve, SBA-15, has been successfully synthesized with a highly ordered two-dimensional P6mm hexagonal mesoporous silica structure and large one-dimensional channels.[14,15] The large sizes of the channels in SBA-15 can reach up to 30 nm. This pore size is ideally suited for the formation of semiconductor quantum structures. Silver-modified zeolites and silver halide (I-VII semiconductor) encapsulated zeolites have a great potential to be applied for chemical synthesis of monodispersed nanostructures, quantum electronics and nonlinear optics, information storage and ion conductors, fast-ion conductors, semiconductors, photoconductors materials, etc.[16,17]

In the present work, a heat diffusion method is used to prepare (SBA-15)-AgI host-guest nanocomposite materials. The as-prepared (SBA-15)-AgI samples were characterized by powder X-ray diffraction, nitrogen adsorption-desorption at 77 K, and solid diffuse reflectance absorption spectra. The X-ray diffraction results showed that the prepared host-guest nanocomposite materials (SBA-15)-AgI still retain the framework of SBA-15, where the channels of SBA-15 were used as the nanometer template. The decrease in pore volume, surface area, and pore diameter of SBA-15 in the host-guest (SBA-15)-AgI through the nitrogen adsorption investigation at 77 K indicated that AgI was confined in the channels of the SBA-15 molecular sieve. The solid diffuse reflectance absorption spectra showed that the absorption of the material is blue-shifted as the loading of AgI guest decreases. We have also investigated the photoluminescence (PL) of the prepared samples. The decrease of the PL intensities upon loading AgI

Dedicated to Professor Fa-Ching Chen on the occasion of his ninetieth birthday.

* Corresponding author. E-mail: nmra@po.iams.sinica.edu.tw
[+] Present address: Institute of Physical Chemistry, Department of Chemistry, Xiamen University, Fujian 361005, P. R. China

in the channels of SBA-15 indicates the change of hydrogen concentration on the pore surface structures of a SBA-15 molecular sieve.

EXPERIMENTAL

Sample Preparation

The sample of mesoporous siliceous SBA-15 molecular sieve was obtained from the synthesis method presented in the literature.[18] The material was calcined in static air at 823 K for 24 h to decompose the triblock copolymer, and a white powder, mesoporous siliceous SBA-15 molecular sieve, was obtained. This material was used as the host to produce the host-guest nanocomposite materials, which are designated as (SBA-15)-AgI. Before the host was used, it was dehydrated at 673 K for 2 h to ensure the removal of the adsorbed water. Silver iodide (99%, New Jersey) was used as received. The mixtures of SBA-15 molecular sieve and AgI were heated at 773 K for 48 h. The sample analyses for silicon by spectrophotometry[19] and for silver by atomic absorption spectrometry were made in order to define the exact compositions of the prepared materials. The host-guest nanomaterials were light yellow.

Characterization

X-ray Diffraction

Powder X-ray diffraction (XRD) was carried out on a Philips X-Pert diffractometer with Cu-$K_{\acute{a}}$ radiation operating at 40 kV and 25 mA for small angles (0.40-10.0 degree) with 0.02 step size and 2 s step time.

Chemical Analysis

The amount of silver was determined by a Hitachi Z-8000 polarized zeeman atomic absorption spectrophotometer. The analyses of silicon were carried out according to molybdosilicate blue photometry.[19]

N_2 Adsorption

Adsorption experiments were carried out on a Coulter SA3100 apparatus. Surface area and pore volumes were determined at 77 K using nitrogen with a conventional volumetric method. Before the analysis, the previously calcined samples were oven dried prior to evacuation overnight at 200 °C for 12 h under vacuum. The surface area was calculated with the BET method based on adsorption data. The calculation of pore size distribution was made using the Barrett-Joyner-Helanda (BJH) method for the adsorption data of the nitrogen sorption isotherms.

DRS-UV Spectra

Diffuse reflectance absorption spectra were recorded with a Hitachi U-3410 visible spectrophotometer. Light sources for the diffuse reflection measurements were tungsten-halogen incandescent and deuterium lamps for low and high energy regions, respectively. Barium sulfate was taken as a standard background.

Luminescence Measurements

The experiment for measuring the PL from SBA-15 and (SBA-15)-AgI samples excited by a pulsed laser are similar to those described previously.[20-23] The SBA-15 and (SBA-15)-AgI (containing 5% and 15% AgI) powders were pressed into pellets prior to the PL measurements performed in a vacuum chamber at 13 K. The samples were excited with an ArF pulsed laser (λ_{exc} = 193 nm; Lambda Physik, Complex 102) with a 10 Hz repetition rate and pulse duration of 25 ns. The laser beam was focused by a 15 cm lens into a 0.03 cm^2 spot. The sample was placed on a copper holder and oriented 45° to the laser beam. The PL was collected in a conventional 90° geometry using a 50 cm SpectraPro-500 monochromator (Acton Res. Corp.) with a 1200 lines/mm grating. The slit width of the monochromator was ~ 0.7 mm. The spectra were recorded by a charge coupled device camera (Princeton Instruments, 330 × 1100 pixels) within an exposure time of 2 s. The data acquisition was processed in a computer equipped with a CSMA software (Princeton Instruments). A set of color filters was used in order to cut the stray radiation from laser and the scattered laser light from the sample.

RESULTS AND DISCUSSION

The small-angle X-ray diffraction of a SBA-15 molecular sieve is shown in Fig. 1, where a well-resolved pattern with a prominent peak is at a 2θ value of 0.9 and the other two peaks are at 1.5 and 1.8. It is typical for a relatively well-ordered material with an intense (1 0 0) diffraction peak and two higher order (1 1 0) and (2 0 0) peaks. The d spacing of calcined SBA-15 molecular sieve is 96.1 Å corresponding to a lattice parameter of 111.0 Å. This agrees with the previously reported results of SBA-15,[24-27] and also confirms the successful synthesis of a SBA-15 molecular sieve. The small angle XRD patterns of the prepared host-guest nanocomposite samples were also performed. Compared with the intensity of calcined SBA-15, the intensities of (SBA-15)-AgI decreased with the loading of the guest AgI. As the guest

loading increased from 10 to 15% (Fig. 1b, c) the intensity of (1 0 0) peak dropped drastically which may be due to the loss of crystallinity of parent material. But in the case of 10% AgI, the loading structure remained as is seen from Fig. 1b. This indicates the reduction of the crystallinity of SBA-15 host due to the incorporation of AgI. But the characteristic diffraction peaks (100) of SBA-15 in the (SBA-15)-AgI still remained (Fig. 1b), thus indicating the structure of the SBA-15 was not destroyed at 10wt% of AgI loading.[28,29] It was found from previous work that the maximum loading, namely the critical dispersion capacity, of the encapsulation of the guest in the pore of SBA-15 was 15.0 wt%.[30] As the encapsulation of AgI increases in the channels of the host SBA-15 molecular sieves disorder of the guest increases thus causing a fall in Gibbs free energy.

The properties of nitrogen adsorption and desorption for the (SBA-15)-AgI and SBA-15 at 77 K were investigated. A nitrogen isotherms of the samples are shown in Fig. 2, where the isotherms can be classified as the type IV isotherm according to the IUPAC nomenclature,[31,32] and the (SBA-15)-AgI host-guest nanocomposites are typical mesoporous materials. Nitrogen adsorption isotherm from (SBA-15)-AgI is quite similar to that from SBA-15, but the overall N_2 adsorption amount decreases. A linear increase of absorbed volume is followed by a sharp increase in nitrogen uptake at relative pressure of $0.65 < P/P_0 < 0.80$, which is due to capillary condensation inside the mesopores,[33] and the sharpness of the step indicates the uniformity of the mesopore size distribution. The BJH (Barret-Joyner-Halenda) method was used to calculate the pore size distribution. The BJH pore size distributions calculated from the adsorption branch of the isotherms with the Kelvin equation[34,35] are presented as the BJH plots in Fig. 3. The results indicate that the distribution of the

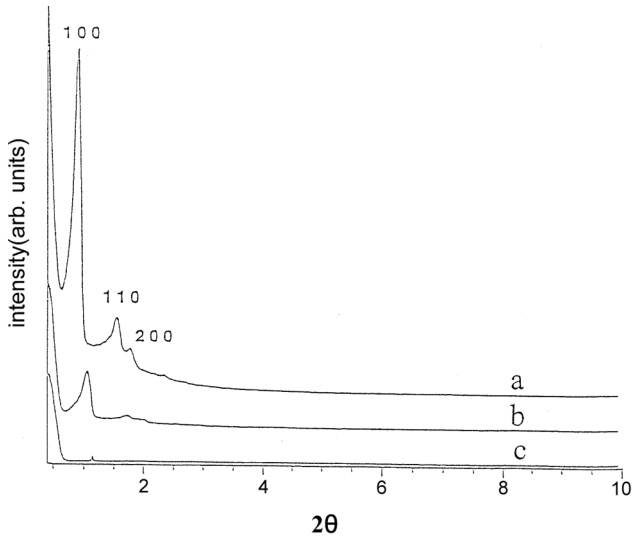

Fig. 1. Small angle XRD patterns of SBA-15 molecular sieve and nanocomposite materials (SBA-15)-AgI: (A) calcined SBA-15 molecular sieve (B) nanocomposite material (SBA-15)-AgI with 10.0 wt% AgI (C) nanocomposite material (SBA-15)-AgI with 15.0 wt% AgI.

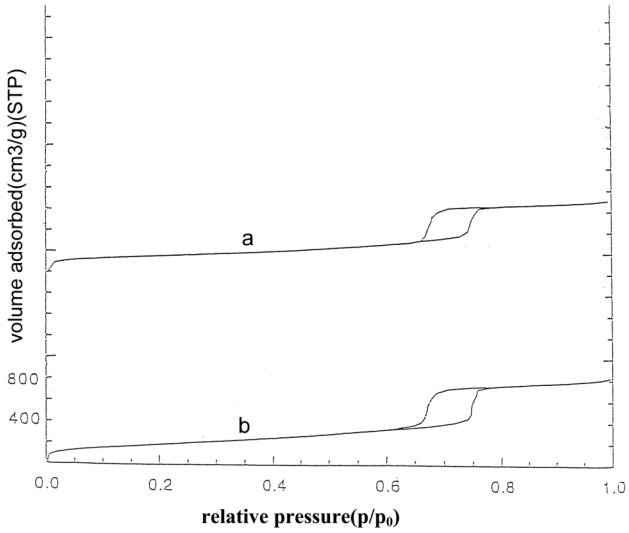

Fig. 2. Nitrogen adsorption-desorption isotherms at 77 K of: (A) (SBA-15)-AgI with 5.0 wt% AgI (B) SBA-15 (The vertical scale is given for the isotherm of SBA-15; the baseline of curve A is displaced vertically to avoid overlap). p: vapour pressure of nitrogen and p_0: Saturated vapour pressure.

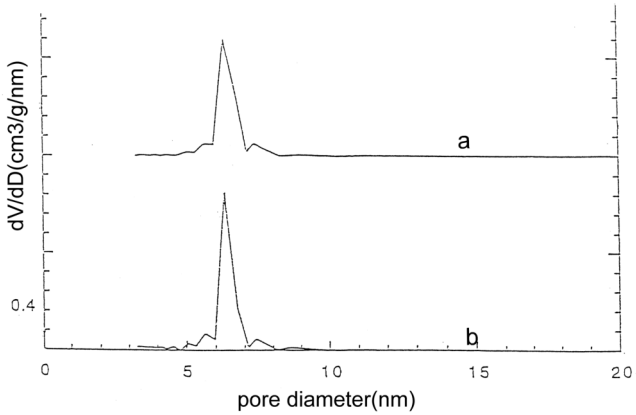

Fig. 3. Pore size distribution curves determined from Barrett-Joyner-Halenda (BJH) formula: (A) (SBA-15)-AgI with 5.0 wt% AgI (B) SBA-15 (The vertical scale is given for the isotherm of SBA-15; the baseline of curve A is displaced vertically to avoid overlap).

pore sizes is very narrow for SBA-15 that has a pore volume and surface area of 1.14 mL/g and 652 m^2/g, respectively. It is interesting to note that the pore volume of the host SBA-15 decreases to 0.905 mL/g and the surface area decreases to 616 m^2/g at the level of 5 wt% loading. The decreases in the pore volume and surface area of the (SBA-15)-AgI sample with 5.0 wt% AgI are 20.6% and 5.5%, respectively, compared with those of the host SBA-15. The pore diameter of SBA-15 decreases by 6.2% from 67.6 Å of the SBA-15 to 63.4 Å for the sample with 5.0 wt% AgI loading. The adsorption investigation indicates that the decrease in the pore volume, surface area and pore diameter of SBA-15 in the host-guest (SBA-15)-AgI composite material results from the incorporation of AgI into the SBA-15, where the AgI predominantly locates in the channels of the SBA-15 when the host-guest composite material was prepared.

The diffuse reflectance spectra (Fig. 4) were obtained using a Hitachi U-3410 spectrophotometer. We prepared different materials with different guest loadings, and observed their solid diffuse reflectance absorption spectra. The results show that the host SBA-15 does not have any absorption in the investigated range of 400-800 nm. In addition, no absorption due to silver oxide was observed at the wavelengths studied, indicating that there is no interaction between silver and the oxygen of the zeolite framework. This absorption originates from the electronic transitions of the isolated molecules in AgI quantum dots. For the sample of (SBA-15)-AgI with 1 wt% AgI, the absorption threshold locates at 2.73 eV (Table 1). But for the sample of (SBA-15)-AgI with 5 wt% AgI, the maximum absorption is at 2.71 eV. More interestingly, as the guest loading increases to 10 wt% even up to 15 wt%, the absorption thresholds move to 2.66 eV and 2.62 eV, respectively. The change in the absorption of the prepared host-guest nanocomposites (SBA-15)-AgI (Table 1) shows that the absorption thresholds are red-shifted as the guest loading increases. Because the channels of the host have a confinement effect on the AgI, quantum confinement[36,37] for both electrons and holes of AgI was enforced by the cluster boundary. In this situation, the nano AgI in the channel of SBA-15 was in the form of zero-dimensional quantum dots or one-dimensional quantum wires. AgI guest was incorporated into the inner surface of the channels of SBA-15. The nano clusters were formed by the interaction among the AgI molecules. The wave functions of electron and hole were expanded in the clusters. The electron-hole excitation energy decreases as the cluster size increases. It is found that the absorption of a sample with low concentration of loading shows a strong absorption. It is expected that in such a sample with a lower concentration of guest, the isolated molecules or quantum dots of AgI are dominant, and the optical transition takes place between the equivalent quantum states and has the same transition probability. But the total oscillator strength is proportional to the number of molecules. In this case, the polariton effect of Frenkel excitons decreases and hence the absorption coefficients of these materials increase.

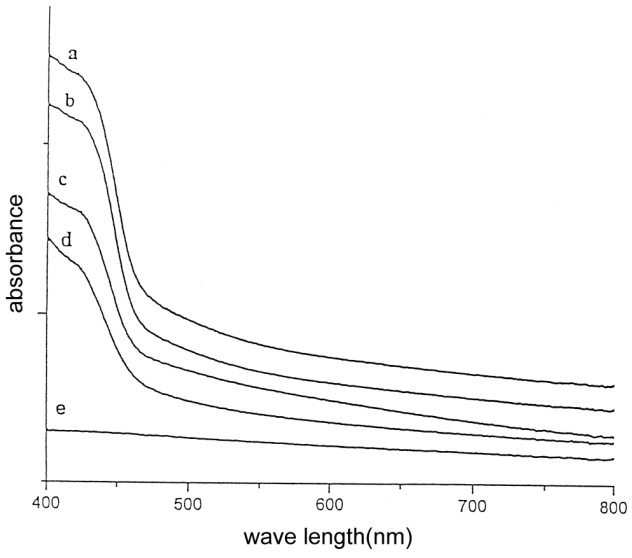

Fig. 4. Diffuse reflectance absorption spectra of (SBA-15)-AgI and SBA-15: (A) (SBA-15)-AgI with 1 wt%AgI (B) (SBA-15)-AgI with 5 wt% AgI (C) (SBA-15)-AgI with 10 wt%AgI (D) (SBA-15)-AgI with 15 wt%AgI (E) SBA-15.

Table 1. DRS-UV Results of (host) SBA-15 with Different (guest) AgI Loadings

Sample (mass percent of AgI)	Threshhold value (eV)	Absorption peak value (nm)
SBA-15-AgI(1wt%)	2.73	455
SBA-15-AgI(5wt%)	2.71	458
SBA-15-AgI(10wt%)	2.66	466
SBA-15-AgI(15wt%)	2.62	474

The PL spectra of SBA-15 and (SBA-15)-AgI (containing 5 wt% and 15 wt% AgI) samples excited by an ArF laser are shown in Fig. 5. The peaks around 2.38 eV have strong PL intensities. In our previous PL studies on SiO_2 nanoparticles and MCM-41 mesoporous silica, the bands with emission at ~2.35 eV were assigned as due to hydrogen-related species on the surface of SiO_2 constituents. While there were vibrational progressions, such as Si-H bending and interfacial H_2O bending observed previously in the PL spectra of siliceous nanoparticles and MCM-41,[20,22,23] the peaks at 2.16 and 2.51 eV in Fig. 5 have energy spacings of 1774 and 1084 cm^{-1}, re-

spectively, to the peak at 2.38 eV. Whether these bands are associated with interfacial H_2O bending progression requires further investigation. The peak at 2.76 eV is attributed to the emission of self-trapped exciton (STE) generated in the siliceous SBA-15 molecular sieve upon the laser excitation. The measured lifetime of ~1 ms for the STE emission is consistent with the spectral nature of the forbidden triplet-singlet transition in the SiO_2 materials.[38] The PL bands at 1.8-1.9 eV due to non-bridging oxygen[39-42] in the SBA-15 molecular sieve are not observed, indicating the lack of dangling bond of Si-O· in the SiO_2 framework at room temperature (Fig. 5). The PL at ~2.38 eV associated with the hydrogen-related species decreases substantially after packing AgI in the channels of SBA-15 molecular sieve. The PL decreases as the AgI loading increases. The prominent reduction in the PL intensity at ~2.38 eV indicates a substantial decrease of the hydrogen concentration on the wall surface in the internal pores of SBA-15 after the loading of AgI. The decrease of the PL intensity at 2.76 eV also suggests a hindrance for generating the STE upon adding AgI into the channels of the SBA-15 molecular sieve. The studies for the dependences of this STE emission on temperature and laser excitation power will be discussed in a future publication.

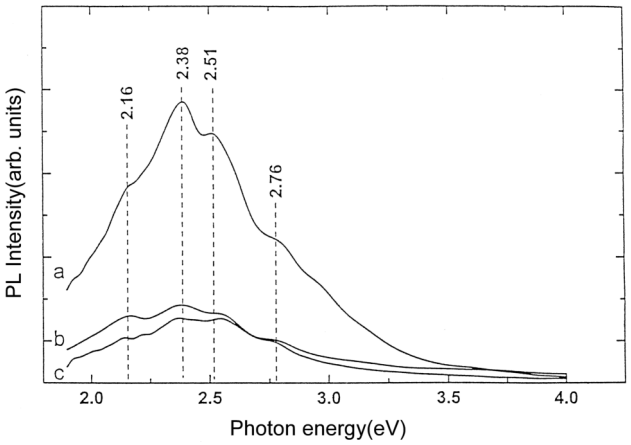

Fig. 5. Photoluminescence spectra of: (A) SBA-15 (B) (SBA-15)-AgI with 10 wt% AgI (C) (SBA-15)-AgI with 15 wt% AgI. The samples were excited with an ArF pulsed laser (λ_{exc} = 193 nm; with a 10 Hz repetition rate and duration of 25 ns. The PL was collected in a conventional 90° geometry using a 50 cm monochromator with a 1200 lines/mm grating. The slit width of the monochromator was ~ 0.7 mm. The spectra were recorded by a charge coupled device camera within an exposure time of 2 s at room temperature.

CONCLUSION

The present work shows that the AgI clusters have been encapsulated in the channels of a SBA-15 molecular sieve with a heat diffusion method. Powder X-ray diffraction indicates that the framework of SBA-15 remained after the loading of AgI guest in the (SBA-15) samples. The nitrogen adsorption-desorption at 77 K investigation indicates that the AgI clusters are confined in the channels of SBA-15. As the guest loading decreases, the maximum absorption of the (SBA-15)-AgI materials in diffuse reflectance absorption is blue-shifted, which can be attributed to a quantum confinement in the channels of SBA-15. Also, it proves that the AgI is located in the channels of the SBA-15 molecular sieve. The PL at ~2.38 eV decreases substantially after the loading of AgI in SBA-15, indicating a great decrease of the hydrogen concentration on the pore surface of SBA-15 after the loading of AgI. The decrease of the STE band at 2.76 eV also suggests a hindrance for generating the excitons upon adding AgI into the channels of the SBA-15 molecular sieve.

Received September 16, 2002.

REFERENCES

1. A special section, *Science* **1990,** *254*, 1300-13341.
2. Breck, D.W. *Zeolite Molecular Sieves: Structure, Chemistry and Use*; Wiley and Sons: London, 1974.
3. Moller, K.; Bein, T. *Chem. Mater.* **1998**, *10*, 2950.
4. Srdanov, V. I.; Alxneit, I.; Stucky, G. D.; Reaves, C.M.; Denbears, S. P. *J. Phys. Chem.* **1998**, *B*, *102*, 3341.
5. Agger, J. R.; Anderson, M. W.; Pemble, M. E.; Terasaki, O.; Nozue, Y. *J. Phys. Chem.* **1998**, *B, 102,* 3345.
6. Perala, H.; Winkler, H.; Kolbe, M.; Wohlfart, A.; Fischer, R. A.; Schmechel, R.; von Seggem, H. *Adv. Mater.* **2000**, *12*, 1050.
7. Liu, Z.; Sakamoto, Y.; Ohsuna, T.; Hiraga, K.; Terasaki, O.; Ko, C. H.; Shin, H. J.; Ryoo, R. *Angew. Chem. Int. Ed.* **2000**, *39*, 3107.
8. Zhang, W.-H.; Shi, J.-L.; Wang, L.-Z.; Yan, D.-S. *Chem. Mater.* **2000**, *12*, 1408.
9. Jang, J.; Lim, B.; Lee, J.; Hyeon, T. *Chem. Comm.* **2001**, 83.
10. Wu, C.-G.; Bein, T. *Science* **1994**, *266,* 1013.
11. Herron, N.; Wang, Y.; Eddy, M. M.; Stucky, G. D.; Cox, D. E.; Moller, K.; Bein, T. *J. Am. Chem. Soc.* **1989**, *111,* 530.
12. Wang, Y.; Herron, N. *J. Phys. Chem.* **1987**, *B, 91,* 257.
13. Hirai, T.; Okubo, H.; Komasawa, I. *J. Phys. Chem.* **1999**, *B, 103,* 4228.
14. Zhao, D.; Feng, J.; Huo, Q.; Melosh, N.; Fredrickson, G. H.;

Chmelka, B. F.; Stucky, G. D. *Science* **1998**, *279,* 548.
15. Zhao, D.; Huo, Q.; Feng, J.; Chmelka, B. F.; Stucky, G. D. *J. Am. Chem. Soc.* **1998**, *120,* 6024.
16. Stein, A.; Ozin, G. A.; Stucky, G. D. *J. Am. Chem. Soc.* **1990**, *112,* 904.
17. Hirono, T.; Yamada, T. *Kokai Tokkyo Koho JP*, Jpn, **1986,** *61 61 894, 8661 894.*
18. Luan, Z.; Hartmann, M.; Zhao, D.; Zhou, W.; Kevan, L. *Chem. Mater.* **1999**, *11,* 1621.
19. Zhai, Q.-Z.; Kim, Y.; Zhang, Z.; Shao, Z.; Xiao, F.; Qiu, S. *Chin. J. Spectr. Lab.* **1998**, *15,* 82.
20. Glinka, Y. D.; Lin, S. H.; Chen, Y.-T. *Appl. Phys. Lett.* **1999,** *75,* 778.
21. Glinka, Y. D.; Lin, S. H.; Chen, Y.-T. *Phys. Rev.* **2000,** *B, 62,* 4733.
22. Glinka, Y. D.; Lin, S. H.; Hwang, L.-P.; Chen, Y.-T. *J. Phys. Chem.* **2000**, *B, 104*, 8652.
23. Glinka, Y. D.; Lin, S. H.; Hwang, L. P.; Chen, Y.-T. *Appl. Phys. Lett.* **2000**, *77,* 3968.
24. Zhao, D.; Feng, J.; Huo, Q.; Melosh, N.; Fredrickson, G. H.; Chmelka, B. F.; Stucky, G. D. *Science* **1998**, *279*, 548.
25. Zhao, D.; Huo, Q.; Feng, J.; Chmelka, B. F.; Stucky, G. D. *J. Am. Chem. Soc.* **1998,** *120,* 6024.
26. Luan, Z.; Hartmann, M.; Zhao, D.; Zhou, W.; Kevan, L. *Chem. Mater.* **1999**, *11,* 1621.
27. Morey, M. S.; O'Brien, S.; Schwarz, S.; Stucky, G. D. *Chem. Mater.* **2000**, *12,* 898.
28. Zhang, W.; Froba, M.; Wang, J.; Tanw, P. T.; Wang, J.; Pinnavaia, T. J. *J. Am. Chem. Soc.* **1996**, *118,* 9164.
29. Xie, Y.; Tang, Y. *Adv. Catal.* **1990**, *37*, 1.
30. Xiao, F.-S.; Qiu, S.; Zheng, S.; Sun, J.; Yu, R.; Xu, R. *J. Catal.* **1998**, *176,* 474.
31. Zhai, Q.-Z.; Khimyak, Y. Z.; Klinowski, J. (unpublished results).
32. IUPAC, Reporting Physisorption Data for Gas/Solid System. *Pure Appl. Chem*. **1957**, *87*, 603.
33. Sing, K. S. W.; Everett, D. H.; Haul, R. A. W.; Moscow, L.; Pierotti, R. A.; Rouquerol, J.; Siemieniewska, T. *Pure. Appl. Chem.* **1985**, *57,* 603.
34. Grun, M.; Lauer, I.; Unger, K. K. *Adv. Mater.* **1997**, *9,* 254.
35. Tanev, P. T.; Vlaev, L. T. *J. Colloid Interface Sci*. **1993**, *160*, 110.
36. Luan, Z.; He, H.; Zhou, W.; Cheng, C. F.; Klinowski, J. *J. Chem. Soc*. **1995**, Faraday.
37. Brus, L. E. *J. Chem. Phys.* **1984***, 80,* 4403.
38. Nagamune, Y.; Takeyams, S.; Miura, Z. *Phys. Rev.* **1989,** *B, 40,* 8099.
39. Itoh, C.; Tanimura, K.; Itoh, M.; Itoh, N. *Phys. Rev.* **1989**, *B, 39,* 11183.
40. Griscom, D. L. *J. Ceramic Society of Japan* **1991**, *99*, 923.
41. Skuja, L.; Tanimura, K.; Itoh, N. *J. Appl. Phys.* **1996**, *80*, 3518.
42. Goldberg, M.; Fitting, H.-J.; Trukhin, A. *J. Non-Cryst. Solids* **1997***, 220,* 69.